

The non-linear energy stability of Brinkman thermosolutal convection with reaction

Bushra Al-Sulaimi¹

Received: 30 November 2015 / Revised: 18 December 2015 / Published online: 4 February 2016
© The Author(s) 2016. This article is published with open access at Springerlink.com

Abstract We use the energy method to obtain the non-linear stability threshold for thermosolutal convection porous media of Brinkman type with reaction. The obtained non-linear boundaries for different values of the reaction terms are compared with the relevant linear instability boundaries obtained by Wang and Tan (Phys Lett A 373:776–780, 2009). Using the energy theory we obtain the non-linear stability threshold below which the solution is globally stable. The compound matrix numerical technique is implemented to solve the associated system of equations with the corresponding boundary conditions. Two systems are investigated, the heated below salted above case and the heated below salted below case. The effect of the reaction terms and Brinkman term on the Rayleigh number is discussed and presented graphically.

Keywords Porous media · Brinkman model · Thermosolutal convection · Energy method · Non-linear stability

Mathematics Subject Classification 76E06 · 76V05 · 35B35

1 Introduction

Convection in porous media has attracted the attention of many researchers and has been an area of great interest in addition to its wide range of applications. Thermal convection in porous media and stability analysis returns back to Horton and Rogers [2], Lapwood [3] and Nield and Barletta [4]. The problem of double-diffusive convection in porous media is well investigated by Nield [5], Rudraiah et al. [6], Wollkind and Frisch [7, 8], Nield and Bejan [9], Ingham and Pop [10, 11], Vafai [12, 13] and

✉ Bushra Al-Sulaimi
b.h.s.al-sulaimi@durham.ac.uk

¹ Department of Mathematical Sciences, University of Durham, Durham DH1 3LE, UK

Vadasz [14]. Bdzil and Frisch [15] performed a linear stability analysis where the fluid catalysed at the lower boundary of the layer and they developed their work in Bdzil and Frisch [16] and a similar work carried by Gutkiewicz-Krusin and Ross [17]. Many recent studies in double and multi-component convection are accomplished by Rionero [18–21]. The first study on the reactive convection in porous media was due to Steinberg and Brand [22, 23]. More studies were carried out by Gatica et al. [24, 25], Viljoen et al. [26] and Malashetty and Gaikwad [27]. Pritchard and Richardson [28] figured out a model similar to that of Steinberg and Brand [22, 23]. They considered the Darcy model to study the onset of thermosolutal convection using linear instability technique. Wang and Tan [1] extended the previous work of Pritchard and Richardson [28] in which Wang and Tan [1] considered Darcy-Brinkman model and used normal mode analysis to carry out a linear instability analysis.

We are studying nonlinear stability using an energy stability method. This method is being used extensively by many leading mathematicians, see for example, Straughan [29, 30], Rionero [31], Capone et al. [32], Straughan [33], Capone and De Luca [34], Rionero and Torricollo [35], Capone et al. [36], Lombardo and Mulone [37], Rionero [38], De Luca [39] and De Luca and Rionero [40]. The work in this paper may be considered as an extension of Wang and Tan [1] and Pritchard and Richardson [28]. Al-Sulaimi [41] used the energy method to carry out a nonlinear stability analysis of Darcy thermosolutal convection with reaction. In this article, the energy stability of Brinkman thermosolutal convection with reaction is considered. The compound matrix numerical technique is used to solve the associated system of equations with the corresponding boundary conditions. Two systems are investigated separately, the heated below-salted above system and the heated below-salted below system. The energy stability boundaries obtained for different values of the reaction rates are compared with the relevant linear instability boundaries. Some linear instability boundaries are obtained by Wang and Tan [1], but they do not correspond directly to what we require and hence we recompute also the linear values using the D^2 Chebyshev tau method.

The aim of the study is to obtain the nonlinear stability boundaries below which the solution is globally stable by using the energy method and compare the nonlinear boundaries with the relevant linear instability boundaries obtained by Wang and Tan [1]. Considering a porous medium of Brinkman type occupying a bounded three-dimensional domain, the variation of the onset of thermosolutal convection with the reaction rate and Brinkman coefficient is discussed.

2 Basic equations

Our model consists of the Brinkman equation with the density in the buoyancy term depends linearly on the temperature T and salt concentration C , the continuity equation, the advection–diffusion equation for the transport of heat and the equation for the transport of solute with reaction terms,

$$p_{,i} = -\frac{\mu}{K}v_i - \rho_0[1 - \alpha_T(T - T_0) + \alpha_C(C - C_0)]gk_i + \lambda\Delta v_i,$$

$$v_{i,i} = 0,$$

$$\begin{aligned}\frac{1}{M}T_{,t} + v_i T_{,i} &= k_T \Delta T, \\ \hat{\phi} C_{,t} + v_i C_{,i} &= \hat{\phi} k_C \Delta C + \hat{k}[f_1(T - T_0) + f_0 - C].\end{aligned}\quad (1)$$

Here v_i , p , T , C are the velocity, pressure, temperature and salt concentration. K is the matrix permeability, μ is the fluid viscosity, ρ_0 is the fluid density. k_C , k_T are the molecular diffusivity of the solute through the fluid and the effective diffusivity of the heat through the saturated medium. M is the ratio of the heat capacity of the fluid to the heat capacity of the medium, $\hat{\phi}$ is the matrix porosity, \hat{k} is the reaction coefficient and $f_0 + f_1(T - T_0) = C_{eq}(T)$ in Pritchard and Richardson [28], where f_0 , f_1 and T_0 are constants. Moreover, g is the gravity, $\mathbf{k} = (0, 0, 1)$ and α_T and α_C are the thermal and solutal expansion coefficients respectively. The symbol Δ is the Laplace operator. The Eq. (1) are taken in the domain $\mathbb{R}^2 \times (0, d) \times \{t > 0\}$. The boundary conditions are

$$\begin{aligned}v_i &= 0 \text{ on } z = 0, d, \\ T &= T_L \text{ on } z = 0, \quad T = T_U \text{ on } z = d, \\ C &= C_L \text{ on } z = 0, \quad C = C_U \text{ on } z = d,\end{aligned}\quad (2)$$

where T_L , T_U , C_L , C_U all constants, with $T_L > T_U$ since our systems are heated below. For the salted above porous medium $C_U > C_L$ while for the salted below case $C_L > C_U$. In the steady state, we look for

$$\begin{aligned}\bar{v}_i &= 0, \\ \bar{T} &= \bar{T}(z), \\ \bar{C} &= \bar{C}(z).\end{aligned}\quad (3)$$

Assuming $C_{eq}(\bar{T}(z)) = \bar{C}(z)$ (see Pritchard and Richardson [28] and Al-Sulaimi [41]), we find the steady solution or the basic state to (1) which we are interested in studying its stability and which satisfies (2) as

$$\begin{aligned}\bar{v}_i &= 0, \\ \bar{T}(z) &= -\beta_T z + T_L, \\ \bar{C}(z) &= -\beta_C z + C_L,\end{aligned}\quad (4)$$

where $\beta_T = (T_L - T_U)/d$ and $\beta_C = (C_L - C_U)/d$ are the temperature and salt gradients respectively.

To analyze the stability of the solutions (4) we define perturbations (u_i, π, θ, ϕ) such that

$$\begin{aligned}v_i &= \bar{v}_i + u_i, \\ p &= \bar{p} + \pi, \\ T &= \bar{T} + \theta, \\ C &= \bar{C} + \phi\end{aligned}\quad (5)$$

Using these perturbations in Eq. (1) we derive the equations governing (u_i, π, θ, ϕ) as

$$\begin{aligned}\pi_{,i} &= -\frac{\mu}{K}u_i + \rho_0 g k_i \alpha_T \theta - \rho_0 g k_i \alpha_C \phi + \lambda \Delta u_i, \\ u_{i,i} &= 0, \\ \frac{1}{M}\theta_t + u_i \theta_{,i} &= \beta_T w + k_T \Delta \theta, \\ \hat{\phi} \phi_t + u_i \phi_{,i} &= \beta_C w + \hat{\phi} k_C \Delta \phi + \hat{k} f_1 \theta - \hat{k} \phi,\end{aligned}\quad (6)$$

where $w = u_3$. To non-dimensionalize the system (6), we define the length, time and velocity scales, L , τ and U , by $L = d$, $\tau = d/MU$ and $U = k_T/d$. We introduce pressure, temperature and salt scales as

$$P = \frac{U d \mu}{K}, \quad T^\# = \frac{\mu \beta_T k_T}{\alpha_T \rho_0 g K}, \quad C^\# = \frac{\mu \beta_C k_T L e}{\alpha_C \rho_0 g K \hat{\phi}},$$

where $Le = k_T/k_C$ is the Lewis number. The temperature and salt Rayleigh numbers are defined as

$$\begin{aligned}R &= \sqrt{\frac{\beta_T d^2 K \alpha_T \rho_0 g}{k_T \mu}}, \\ R_s &= \sqrt{\frac{\beta_C d^2 K \alpha_C \rho_0 g L e}{\hat{\phi} k_T \mu}} \quad \text{when } C_L > C_U \quad \text{or} \quad R_s = \sqrt{\frac{|\beta_C| d^2 K \alpha_C \rho_0 g L e}{\hat{\phi} k_T \mu}} \quad \text{when} \\ &\quad C_L < C_U.\end{aligned}$$

Then, the fully nonlinear, perturbed dimensionless form of (6) is

$$\begin{aligned}\pi_{,i} &= -u_i + R k_i \theta - R_s k_i \phi + \tilde{\gamma} \Delta u_i, \\ u_{i,i} &= 0, \\ \theta_{,t} + u_i \theta_{,i} &= R w + \Delta \theta, \\ \varepsilon \phi_{,t} + \frac{L e}{\hat{\phi}} u_i \phi_{,i} &= \mp R_s w + \Delta \phi + h \theta - \eta \phi,\end{aligned}\quad (7)$$

where $\varepsilon = M L e$, $\tilde{\gamma} = \lambda K / \mu d^2$ the Brinkman coefficient and h and η are the reaction terms

$$h = \frac{\hat{k} f_1 d^2 T^\#}{\hat{\phi} k_C C^\#} \quad \text{and} \quad \eta = \frac{\hat{k} d^2}{\hat{\phi} k_C}.$$

Moreover, $+R_s$ is taken for the salted below system and $-R_s$ is taken for the salted above system. The corresponding boundary conditions are

$$Dw = w = \theta = \phi = 0 \quad \text{on } z = 0 \quad \text{and} \quad z = 1. \quad (8)$$

3 Linear instability theory

To study the linear instability, we drop the nonlinear terms of (7) and take the double curl of equation (7)₁ and retaining only the third component of the resulting equation to reduce (7) to studying the system

$$\begin{aligned}\Delta w - R\Delta^*\theta + R_s\Delta^*\phi - \tilde{\gamma}\Delta^2 w &= 0, \\ \theta_{,t} &= R w + \Delta\theta, \\ \varepsilon\phi_{,t} &= \mp R_s w + \Delta\phi + h\theta - \eta\phi,\end{aligned}\tag{9}$$

where Δ^* is the horizontal Laplacian. Assuming a normal mode representation for w , θ and ϕ of the form $w = W(z)f(x, y)$, $\theta = \Theta(z)f(x, y)$ and $\phi = \Phi(z)f(x, y)$ where $f(x, y)$ is a plan tiling function satisfying

$$\Delta^* f = -a^2 f;\tag{10}$$

(see Straughan [29]) and a is a wave number. Using (10) and applying the normal mode representations to (9), we find

$$\begin{aligned}(D^2 - a^2)W + Ra^2\Theta - R_s a^2\Phi - \tilde{\gamma}(D^2 - a^2)^2 W &= 0, \\ \sigma\Theta &= RW + (D^2 - a^2)\Theta, \\ \varepsilon\sigma\Phi &= \mp R_s W + (D^2 - a^2)\Phi + h\Theta - \eta\Phi,\end{aligned}\tag{11}$$

where $D = d/dz$. This is an eigenvalue problem for σ to be solved subject to the boundary conditions

$$DW = W = \Theta = \Phi = 0, \text{ on } z = 0, 1.\tag{12}$$

System (11) with the corresponding boundary conditions (12) is solved using the D^2 Clebshev tau method. Detailed numerical results for the heated below-salted above and heated below-salted below are reported separately in the subsections (6.1) and (6.2). We determine the critical Rayleigh number given by $Ra_L^2 = \min_{a^2} R^2(a^2)$ where for all $R^2 > Ra_L^2$ the system is unstable.

4 Nonlinear energy stability theory

In order to study the nonlinear stability of the Brinkman model for the double diffusive convection, we consider the nonlinear system of equations in the dimensionless form (7) and the corresponding boundary conditions (8). Taking into consideration the periodicity of the system and the smoothness of the boundary to allow the application of the *Divergence Theorem*. Multiply Eq. (7)₁ by u_i and integrate over V using integration by parts. Similarly, multiply Eq. (7)₃ by θ and Eq. (7)₄ by ϕ and integrate. The following

system of energy equations is obtained

$$\begin{aligned} 0 &= -\|\mathbf{u}\|^2 + R(\theta, w) - R_s(\phi, w) - \tilde{\gamma}\|\nabla\mathbf{u}\|^2, \\ \frac{d}{dt}\frac{1}{2}\|\theta\|^2 &= R(\theta, w) - \|\nabla\theta\|^2, \\ \frac{d}{dt}\frac{\varepsilon}{2}\|\phi\|^2 &= \mp R_s(\phi, w) - \|\nabla\phi\|^2 + h(\theta, \phi) - \eta\|\phi\|^2. \end{aligned} \quad (13)$$

Then we form the combination of the equations in system (13) as

$$(13)_1 + (13)_2 + \lambda(13)_3,$$

where λ a coupling parameter. This leads to the energy identity

$$\frac{dE}{dt} = I - D = -D \left(1 - \frac{I}{D}\right), \quad (14)$$

where

$$\begin{aligned} E &= \frac{1}{2}\|\theta\|^2 + \frac{\varepsilon\lambda}{2}\|\phi\|^2, \\ I &= 2R(\theta, w) + \lambda h(\theta, \phi) - (1 \pm \lambda)R_s(\phi, w), \\ D &= \|\mathbf{u}\|^2 + \|\nabla\theta\|^2 + \lambda\|\nabla\phi\|^2 + \lambda\eta\|\phi\|^2 + \tilde{\gamma}\|\nabla\mathbf{u}\|^2. \end{aligned} \quad (15)$$

Then

$$\frac{dE}{dt} \leq -D \left(1 - \max_H \frac{I}{D}\right) = -D \left(1 - \frac{1}{R_E}\right) \quad (16)$$

is an energy inequality which follows from the energy identity, where H is the space of admissible solutions. Namely

$$H = \left\{u_i, \theta, \phi \in H^1(V) : u_i = \theta = \phi = 0 \text{ on } z = 0, 1\right\},$$

and

$$\frac{1}{R_E} = \max_H \frac{I}{D}. \quad (17)$$

The nonlinear stability ensues when $R_E > 1$ which implies that $1 - 1/R_E > 0$.

By using the Poincaré inequality we can show

$$D \geq 2k\pi^2 \left(\frac{\|\theta\|^2 + \lambda\varepsilon\|\phi\|^2}{2} \right) = 2k\pi^2 E, \quad (18)$$

where $k = \min \left\{ \frac{1}{ML_e}, 1 \right\}$. Then from (16) we may derive the inequality

$$\frac{dE}{dt} \leq -2a_1 k \pi^2 E(t),$$

where the coefficient a_1 is defined by

$$a_1 = \frac{R_E - 1}{R_E}.$$

Upon integration we obtain

$$E(t) \leq E(0)e^{-2a_1k\pi^2t}. \quad (19)$$

Inequality (19) shows that under the condition $R_E > 1$, $E(t) \rightarrow 0$ as $t \rightarrow \infty$. This result according to Eq. (15)₁, proves that $\|\theta\|^2 \rightarrow 0$ and $\|\phi\|^2 \rightarrow 0$ as $t \rightarrow \infty$. To show the decay of $\|\mathbf{u}\|$, we have to use the Poincaré inequality, the Arithmetic–Geometric Mean inequality and the fact $\|w\|^2 \leq \|\mathbf{u}\|^2$ in the energy equation (13)₁ to obtain

$$(1 + \tilde{\gamma}\pi^2)\|\mathbf{u}\|^2 \leq \left(\frac{R\alpha}{2} + \frac{R_s\beta}{2}\right)\|\mathbf{u}\|^2 + \frac{R}{2\alpha}\|\theta\|^2 + \frac{R_s}{2\beta}\|\phi\|^2, \quad (20)$$

where α and β are constants to be chosen such that $R\alpha + R_s\beta = 1$, which gives $\alpha = 1/2R$ and $\beta = 1/2R_s$. This leads to

$$\left(\frac{1}{2} + \tilde{\gamma}\pi^2\right)\|\mathbf{u}\|^2 \leq R^2\|\theta\|^2 + R_s^2\|\phi\|^2. \quad (21)$$

Inequality (21) shows that R_E^{-1} guarantees in addition to the decay of $\|\theta\|$ and $\|\phi\|$, also decay of $\|\mathbf{u}\|$.

Turning our attention to the maximization problem (17). We have to solve it by deriving the Euler–Lagrange equations. The maximum problem is

$$\frac{1}{R_E} = \max_H \frac{2R(\theta, w) + \lambda h(\theta, \phi) - R_s(1 \pm \lambda)(\phi, w)}{\|\mathbf{u}\|^2 + \|\nabla\theta\|^2 + \lambda\|\nabla\phi\|^2 + \lambda\eta\|\phi\|^2 + \tilde{\gamma}\|\nabla\mathbf{u}\|^2}. \quad (22)$$

Rescaling ϕ by putting $\tilde{\phi} = \sqrt{\lambda}\phi$. Equation (22) will be

$$\frac{1}{R_E} = \max_H \frac{2R(\theta, w) + \sqrt{\lambda}h(\theta, \tilde{\phi}) - R_s f(\lambda)(\tilde{\phi}, w)}{\|\mathbf{u}\|^2 + \|\nabla\theta\|^2 + \|\nabla\tilde{\phi}\|^2 + \eta\|\tilde{\phi}\|^2 + \tilde{\gamma}\|\nabla\mathbf{u}\|^2}, \quad (23)$$

where

$$f(\lambda) = \frac{1 \pm \lambda}{\sqrt{\lambda}}.$$

The Euler–Lagrange equations for this maximum are

$$\begin{aligned} 2u_i - 2RR_E k_i \theta + R_s R_E f k_i \tilde{\phi} - 2\tilde{\gamma} \Delta u_i &= -R_E P_{,i} \\ -2\Delta\theta - 2R_E R w - \sqrt{\lambda} R_E h \tilde{\phi} &= 0 \\ -2\Delta\tilde{\phi} + 2\eta\tilde{\phi} + R_E R_s f w - \sqrt{\lambda} R_E h \theta &= 0, \end{aligned} \quad (24)$$

where P is a Lagrange multiplier. To remove the Lagrange multiplier, we take the double Curl of equation (24)₁ and retaining only the third component of the resulting equation to reduce (24) to

$$\begin{aligned}\Delta w - RR_E \Delta^* \theta + \left(\frac{1 \pm \lambda}{2} \right) R_s R_E \Delta^* \phi - \tilde{\gamma} \Delta^2 w &= 0, \\ \Delta \theta + R_E R w + R_E \frac{\lambda h}{2} \phi &= 0, \\ (\Delta - \eta) \phi - R_E R_s \left(\frac{1 \pm \lambda}{2\lambda} \right) w + R_E \frac{h}{2} \theta &= 0,\end{aligned}\quad (25)$$

where $\Delta^* = \partial^2/\partial x^2 + \partial^2/\partial y^2$ is the horizontal Laplacian. Introducing the normal mode representation as presented in Sect. 3, system (25) becomes

$$\begin{aligned}(D^2 - a^2)W - \tilde{\gamma}(D^2 - a^2)^2 W + a^2 R_E R \Theta - a^2 R_E R_s \left(\frac{1 \pm \lambda}{2} \right) \Phi &= 0, \\ R_E R W + (D^2 - a^2)\Theta + \left(\frac{h\lambda}{2} \right) R_E \Phi &= 0, \\ R_E R_s \left(\frac{1 \pm \lambda}{2\lambda} \right) W - \frac{h}{2} R_E \Theta + \eta \Phi - (D^2 - a^2)\Phi &= 0.\end{aligned}\quad (26)$$

The Laplace operator is equivalent to $\Delta = D^2 - a^2$, where $D = \partial/\partial z$. The corresponding boundary conditions are

$$DW = W = \Theta = \Phi = 0, \text{ on } z = 0, 1. \quad (27)$$

We can determine the critical Rayleigh number given by $Ra_E^2 = \max_{\lambda} \min_{a^2} R^2(a^2, \lambda)$, where for all $R^2 < Ra_E^2$ the system is stable.

5 Numerical method

We have used the D^2 Chebyshev tau method (Dongarra et al. [42]) to find the bound for the linear instability theory, system (11) and the corresponding boundary conditions (12). For the energy theory we have used the compound matrix technique (Lindsay and Straughan [43]).

5.1 The D^2 Chebyshev tau method for the linear theory

Using the D^2 Chebyshev to solve (11) subject to (12), we have to introduce a variable χ such that $\chi = \Delta w$. Then, Eq. (11) will be

$$\begin{aligned}
 (D^2 - a^2)W - \chi &= 0, \\
 \tilde{\gamma}(D^2 - a^2)\chi - \chi - a^2 R\Theta + a^2 R_s \Phi &= 0, \\
 (D^2 - a^2)\Theta + RW &= \sigma \Theta, \\
 (D^2 - a^2)\Phi - \eta \Phi + h\Theta \mp R_s W &= \varepsilon \sigma \Phi.
 \end{aligned} \tag{28}$$

The functions W , χ , Θ and Φ are expanded in terms of Chebyshev polynomials

$$\begin{aligned}
 W(z) &= \sum_{n=1}^N w_n T_n(z), \quad \chi(z) = \sum_{n=1}^N \chi_n T_n(z), \quad \Theta(z) = \sum_{n=1}^N \theta_n T_n(z), \\
 \Phi(z) &= \sum_{n=1}^N \phi_n T_n(z).
 \end{aligned}$$

Since $T_n(\pm 1) = (\pm 1)^n$ and $T'_n(\pm 1) = (\pm 1)^{n-1}n^2$, implies that the boundary conditions (12) become

$$\begin{aligned}
 w_2 + w_4 + w_6 + \cdots + w_N &= 0, \\
 w_1 + w_3 + w_5 + \cdots + w_{N-1} &= 0
 \end{aligned} \tag{29}$$

with similar representations for θ_n and ϕ_n

$$\begin{aligned}
 \theta_2 + \theta_4 + \theta_6 + \cdots + \theta_N &= 0, \\
 \theta_1 + \theta_3 + \theta_5 + \cdots + \theta_{N-1} &= 0,
 \end{aligned} \tag{30}$$

$$\begin{aligned}
 \phi_2 + \phi_4 + \phi_6 + \cdots + \phi_N &= 0, \\
 \phi_1 + \phi_3 + \phi_5 + \cdots + \phi_{N-1} &= 0,
 \end{aligned} \tag{31}$$

while the boundary condition $Dw = 0$ becomes

$$\begin{aligned}
 2^2 w_2 + 4^2 w_4 + 6^2 w_6 + \cdots + N^2 w_N &= 0, \\
 w_1 + 3^2 w_3 + 5^2 w_5 + \cdots + (N-1)^2 w_{N-1} &= 0
 \end{aligned} \tag{32}$$

Therefore, the Chebyshev tau method reduces to solving the matrix system $A\mathbf{x} = \sigma B\mathbf{x}$, where $\mathbf{x} = (w_1, w_2, \dots, w_N, \chi_1, \chi_2, \dots, \chi_N, \theta_1, \dots, \theta_N, \phi_1, \dots, \phi_N)$ and the matrices A and B are given by

$$A = \begin{pmatrix}
 4D^2 - a^2 I & -I & 0 & 0 \\
 BC1 & 0 \cdots 0 & 0 \cdots 0 & 0 \cdots 0 \\
 BC2 & 0 \cdots 0 & 0 \cdots 0 & 0 \cdots 0 \\
 0 & 4D^2 - a^2 I - \frac{I}{\tilde{\gamma}} & -a^2 R \frac{I}{\tilde{\gamma}} & a^2 R_s \frac{I}{\tilde{\gamma}} \\
 BC7 & 0 \cdots 0 & 0 \cdots 0 & 0 \cdots 0 \\
 BC8 & 0 \cdots 0 & 0 \cdots 0 & 0 \cdots 0 \\
 RI & 0 & 4D^2 - a^2 I & 0 \\
 0 \cdots 0 & 0 \cdots 0 & BC3 & 0 \cdots 0 \\
 0 \cdots 0 & 0 \cdots 0 & BC4 & 0 \cdots 0 \\
 \mp R_s I & 0 & hI & 4D^2 - (a^2 + \eta)I \\
 0 \cdots 0 & 0 \cdots 0 & 0 \cdots 0 & BC5 \\
 0 \cdots 0 & 0 \cdots 0 & 0 \cdots 0 & BC6
 \end{pmatrix}$$

$$B = \begin{pmatrix} 0 & 0 & 0 & 0 \\ 0 \cdots 0 & 0 \cdots 0 & 0 \cdots 0 & 0 \cdots 0 \\ 0 \cdots 0 & 0 \cdots 0 & 0 \cdots 0 & 0 \cdots 0 \\ 0 & 0 & 0 & 0 \\ 0 \cdots 0 & 0 \cdots 0 & 0 \cdots 0 & 0 \cdots 0 \\ 0 \cdots 0 & 0 \cdots 0 & 0 \cdots 0 & 0 \cdots 0 \\ 0 & 0 & I & 0 \\ 0 \cdots 0 & 0 \cdots 0 & 0 \cdots 0 & 0 \cdots 0 \\ 0 \cdots 0 & 0 \cdots 0 & 0 \cdots 0 & 0 \cdots 0 \\ 0 & 0 & 0 & \varepsilon I \\ 0 \cdots 0 & 0 \cdots 0 & 0 \cdots 0 & 0 \cdots 0 \\ 0 \cdots 0 & 0 \cdots 0 & 0 \cdots 0 & 0 \cdots 0 \end{pmatrix}$$

where in the matrix A the notations $BC1$, $BC2$ refer to the boundary conditions (29), $BC3$, $BC4$ refer to (30), $BC5$, $BC6$ refer to (31) and $BC7$, $BC8$ refer to the boundary conditions (32). We solved the matrix system by the QZ algorithm (Dongarra et al. [42]).

5.2 The compound matrix technique for the energy theory

To employ the compound matrix method (Lindsay and Straughan [43]), we have to write system (26) as

$$\begin{aligned} D^4 W &= -a^4 W + 2a^2 D^2 W - \frac{a^2}{\tilde{\gamma}} W + \frac{1}{\tilde{\gamma}} D^2 W + R_E R \frac{a^2}{\tilde{\gamma}} \Theta - \frac{a^2}{\tilde{\gamma}} \left(\frac{1 \pm \lambda}{2} \right) R_E R_s \Phi, \\ D^2 \Theta &= a^2 \Theta - R_E R W - \left(\frac{h\lambda}{2} \right) R_E \Phi, \\ D^2 \Phi &= \left(a^2 + \eta \right) \Phi - \frac{h}{2} R_E \Theta + \left(\frac{1 \pm \lambda}{2\lambda} \right) R_E R_s W. \end{aligned} \quad (33)$$

The compound matrix for (33) works with the 4×4 minors of the 8×4 solution matrix formed from

$$\begin{aligned} U_1 &= (W_1, W_1', W_1'', W_1''', \Theta_1, \Theta_1', \Phi_1, \Phi_1'), \\ U_2 &= (W_2, W_2', W_2'', W_2''', \Theta_2, \Theta_2', \Phi_2, \Phi_2'), \\ U_3 &= (W_3, W_3', W_3'', W_3''', \Theta_3, \Theta_3', \Phi_3, \Phi_3'), \\ U_4 &= (W_4, W_4', W_4'', W_4''', \Theta_4, \Theta_4', \Phi_4, \Phi_4'). \end{aligned} \quad (34)$$

The solutions U_i for $i = 1, 2, 3, 4$ are independent solutions to (33) for different initial values, U_i 's correspond to solutions for starting values

$$\begin{aligned} &(0, 0, 1, 0, 0, 0, 0, 0)^T, \quad (0, 0, 0, 1, 0, 0, 0, 0)^T, \\ &(0, 0, 0, 0, 0, 1, 0, 0)^T, \quad (0, 0, 0, 0, 0, 0, 0, 1)^T, \end{aligned}$$

respectively. We define $C_4^8 = 70$ new variables y_1, \dots, y_{70} as the 4×4 minors. For example

$$y_1 = \begin{vmatrix} W_1 & W_2 & W_3 & W_4 \\ W'_1 & W'_2 & W'_3 & W'_4 \\ W''_1 & W''_2 & W''_3 & W''_4 \\ W'''_1 & W'''_2 & W'''_3 & W'''_4 \end{vmatrix}$$

implies that $y_1 = W_1 W'_2 W''_3 W'''_4 + \dots$, which gives 24 terms for y_1 . So, the idea is to derive y_2, \dots, y_{70} similarly and then obtain differential equations for the y_i 's by differentiation. There is no need to write out the whole determinant each time. The first term, y_1 , suffices. By differentiating each y_i and substituting from Eq. (33) we obtain differential equations for the y_i , cf. Lindsay and Straughan [43] and chapter 19 of Straughan [29]. These equations are integrated numerically from 0 to 1. We keep the boundary conditions (27) at $z = 0$ and replace the ones at $z = 1$ by

$$W''_1(0) = W''_2(0) = \Theta'_3(0) = \Phi'_4(0) = 1, \quad (35)$$

which using the y_i 's yields the initial condition for the y_i 's as

$$y_{60}(0) = 1. \quad (36)$$

Using y_i 's, the final condition which satisfies (27) is seen to be

$$y_{11}(1) = 0. \quad (37)$$

The eigenvalue R is varied until (37) is satisfied to some pre-assigned tolerance.

6 Numerical results and conclusion

6.1 Heated below salted above system

The numerical integration is carried out for different values of the reaction rates, h and η and different values of the Brinkman coefficient $\tilde{\gamma}$. We found that when the layer is heated below and salted above in the case of no reaction i.e. $h = \eta = 0$ and when Brinkman coefficient $\tilde{\gamma} = 1$ that the numerical methods used give exactly the same values for Ra_L and Ra_E . The graphical representation of these values shows that the linear instability threshold coincide with the energy stability threshold as it is clear in Fig. 1a and that there is no region of subcritical instability. As we increase the values of the reaction rates h and η , the linear instability boundary starts to diverge from the energy stability boundary. Figure 1 shows the effect of increasing the values of the reaction rates, as we increase the values of h and η , the gap between the boundaries increases. Any point (Rs^2, Ra^2) in the space above the linear instability boundary, the solid line Ra_L^2 , represents a region where the system is unstable because the linear instability boundary guarantees instability. On the other hand, if (Rs^2, Ra^2) lies below the energy stability boundary, the dashed line Ra_E^2 , represents the space where the system is definitely stable. Note that as the reaction rates increase, the peak

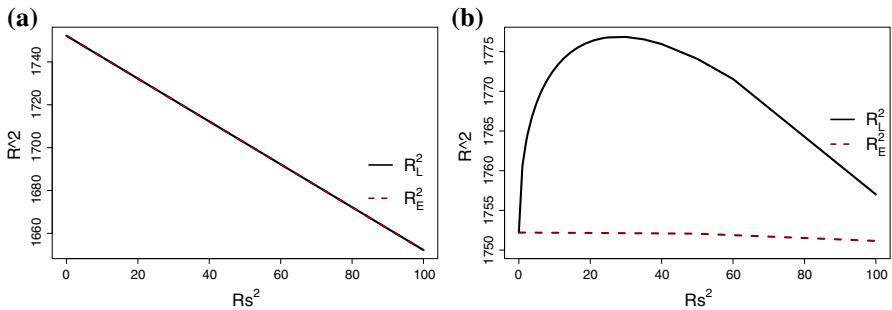


Fig. 1 Linear instability and energy stability boundaries for the salted above Brinkman convection problem for different values of the reaction rates h and η . **a** $h = \eta = 0$. **b** $h = 5, \eta = 3$

Table 1 Some numerical values obtained for the linear boundary Ra_L and energy boundary Ra_E temperature Rayleigh number with corresponding salt Rayleigh number R_s and the corresponding critical wave numbers a_L and a_E when $\tilde{\gamma} = 1, h = 9$ and $\eta = 6$ in the case of heated below salted above system

R_s^2	a_L	Ra_L^2	a_E	Ra_E^2	λ
1	3.13	1766.156	3.12	1752.197	0.055
3	3.13	1775.442	3.12	1752.187	0.099
5	3.14	1781.378	3.12	1752.179	0.132
6	3.14	1783.775	3.12	1752.175	0.146
12	3.15	1794.255	3.12	1752.157	0.220
20	3.15	1803.123	3.12	1752.137	0.304

of the linear instability curve moves to a higher position resulting in a wider region of possible subcritical instability between the energy stability threshold and the linear instability threshold. Moreover, there is a slight noticeable decrease in the energy stability threshold as the values of $R_s \rightarrow +\infty$. Table 1 represents some numerical values obtained.

To study the effect of each one of h and η on the stability of the system, a bigger difference between their values is considered. It has been noticed that when h is bigger compared to η , the region of possible subcritical instability is wider and increasing the value of h implies more divergence of the linear instability boundary from the energy stability boundary and a movement of the peak value of the linear instability threshold to a higher position, as Fig. 2a shows. Compared to the case when η has a bigger value than h , the linear and energy boundaries coincide as shown in Fig. 2b and the linear boundary covers the content of stability. This is expected, as system (7) shows that $h\Theta$ is a destabilizing term while $-\eta\Phi$ is a stabilizing term.

Examining the effect of different values of the Brinkman coefficient (effective viscosity term) on the stability boundaries, reveals that increasing the value of $\tilde{\gamma}$ results in a wider space of global stability below the energy stability threshold and a wider region of potential subcritical instability. The effect of different values of $\tilde{\gamma}$ ($= 0.5, 2$) are presented graphically in Fig. 3.

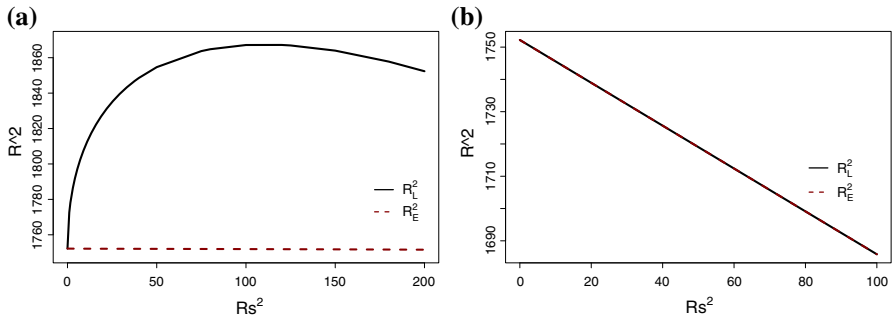


Fig. 2 Linear instability and energy stability boundaries for the salted above Brinkman convection problem. The difference between the values of the reaction rates h and η is large. **a** $h = 10$, $\eta = 0$. **b** $h = 0$, $\eta = 10$

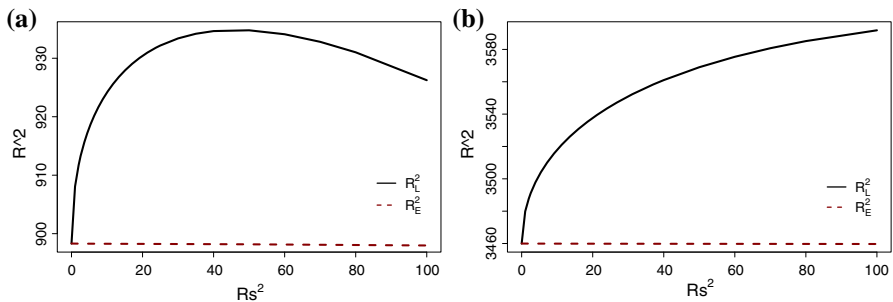


Fig. 3 Linear instability and energy stability boundaries for the salted above Brinkman convection problem for different values of the Brinkman constant when $h = 9$ and $\eta = 6$. **a** $\tilde{\gamma} = 0.5$. **b** $\tilde{\gamma} = 2$

6.2 Heated and salted Below system

It is instructive to write system (7) and the boundary conditions (8) for the salted below case as an abstract equation of form

$$A\mathbf{u}_t = L(\mathbf{u}) + N(\mathbf{u}),$$

where $\mathbf{u} = (u_1, u_2, u_3, \theta, \phi)$, $N(\mathbf{u})$ represents the nonlinear terms in (7) so

$$N(\mathbf{u}) = \begin{pmatrix} 0 \\ 0 \\ 0 \\ -u_i \theta_{,i} \\ -\frac{Le}{\phi} u_i \phi_{,i} \end{pmatrix},$$

and L is the linear operator. In fact, the linear operator for (7) is

$$L = \begin{pmatrix} -1 + \tilde{\gamma}\Delta & 0 & 0 & 0 & 0 \\ 0 & -1 + \tilde{\gamma}\Delta & 0 & 0 & 0 \\ 0 & 0 & -1 + \tilde{\gamma}\Delta & R & -R_s \\ 0 & 0 & R & \Delta & 0 \\ 0 & 0 & R_s & h & \Delta - \eta I \end{pmatrix}.$$

We may split L into a symmetric plus skew-symmetric part as follows

$$L = L_s + L_A,$$

where

$$L_s = \begin{pmatrix} -1 + \tilde{\gamma}\Delta & 0 & 0 & 0 & 0 \\ 0 & -1 + \tilde{\gamma}\Delta & 0 & 0 & 0 \\ 0 & 0 & -1 + \tilde{\gamma}\Delta & R & 0 \\ 0 & 0 & R & \Delta & \frac{h}{2} \\ 0 & 0 & 0 & \frac{h}{2} & \Delta - \eta I \end{pmatrix},$$

and

$$L_A = \begin{pmatrix} 0 & 0 & 0 & 0 & 0 \\ 0 & 0 & 0 & 0 & 0 \\ 0 & 0 & 0 & 0 & -R_s \\ 0 & 0 & 0 & 0 & -\frac{h}{2} \\ 0 & 0 & R_s & \frac{h}{2} & 0 \end{pmatrix}.$$

For the salted above case, the previous subsection, L_A would be zero and the analogous linear operator L would be symmetric. Even when $h = 0$ in the salted below case, we expect some problem with nonlinear energy stability theory since

$$(\mathbf{u}, L(\mathbf{u})) \neq (\mathbf{u}, L_s(\mathbf{u}))$$

where (\cdot, \cdot) is the inner product on $(H^1(V))^5$ with V being a period cell for the solution. For the problem of this subsection, governed by Eqs. (7) and (8) for the salted below case, we have two sources of anti-symmetry, the R_s term and the h term.

The numerical values are presented graphically for different values of the reaction rates h and η in Fig. 4. It has been noticed that as the reaction rate increases, the gap between the linear instability and energy stability boundaries increases due to the divergence of the linear threshold yielding a wider region of potential subcritical instability. Whereas, the energy stability threshold is approximately constant or more precisely it is decreasing unnoticeably as shown in Figs. 4 and 5. As expected from system (7) one sees that $h\Theta$ will destabilize the system while $-\eta\Phi$ will stabilize the system which is clear and shown in Fig. 5 i.e., when the value of h is smaller compared to η the space of possible subcritical instability is less compared to the case when h is larger than η . The effect of changing the value of $\tilde{\gamma}$ can be noticed in Fig. 6 for $\tilde{\gamma} = 0.5, 2$. The gap between the boundaries increases and the space of global stability is wider as $\tilde{\gamma}$ increases.

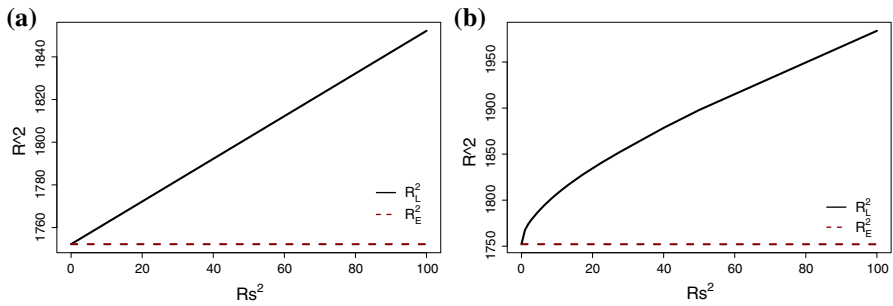


Fig. 4 Linear instability and energy stability boundaries for the salted below Brinkman convection problem for different values of the reaction rates h and η . **a** $h = \eta = 0$. **b** $h = 9$, $\eta = 6$

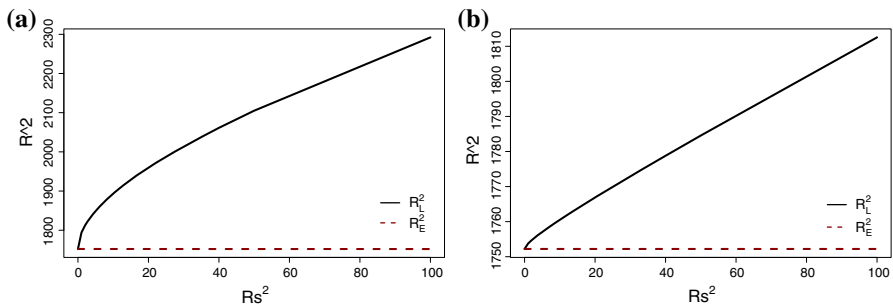


Fig. 5 Linear instability and energy stability boundaries for the salted below Brinkman convection problem. The difference between the values of the reaction rates h and η is large. **a** $h = 20$, $\eta = 1$. **b** $h = 1$, $\eta = 20$

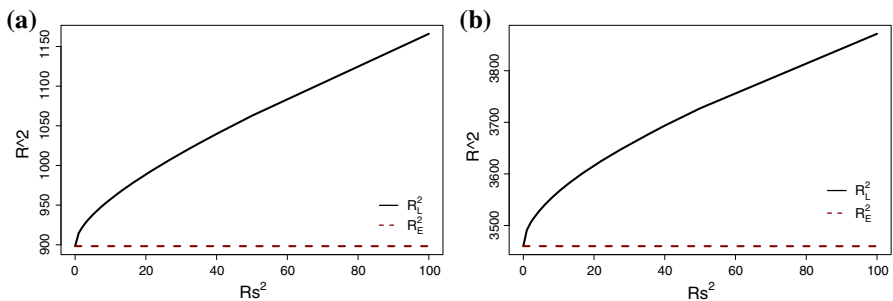


Fig. 6 Linear instability and energy stability boundaries for the salted below Brinkman convection problem for different values of the Brinkman coefficient when $h = 10$ and $\eta = 0$. **a** $\tilde{\gamma} = 0.5$. **b** $\tilde{\gamma} = 2$

The numerical values and their graphical representations show that the linear instability theory does not necessarily represent accurately the onset of convection and we may explain that this is due to the two sources of anti-symmetry the R_s term and the h term. By this we mean that the linear instability boundary is definitely a threshold for instability, but in this case, it may be possible for instability to arise with a Rayleigh number below the linear instability boundary.

Acknowledgments This work is supported by a scholarship from the Ministry of Higher Education, Muscat, Sultanate of Oman. I would like to thank Professor Brian Straughan for his discussion and comments.

Open Access This article is distributed under the terms of the Creative Commons Attribution 4.0 International License (<http://creativecommons.org/licenses/by/4.0/>), which permits unrestricted use, distribution, and reproduction in any medium, provided you give appropriate credit to the original author(s) and the source, provide a link to the Creative Commons license, and indicate if changes were made.

References

1. Wang, S., Tan, W.: The onset of Darcy–Brinkman thermosolutal convection in a horizontal porous media. *Phys. Lett. A* **373**, 776–780 (2009)
2. Horton, C.W., Rogers, F.T.: Convection currents in a porous medium. *J. Appl. Phys.* **16**(6), 367–370 (1945)
3. Lapwood, E.: Convection of a fluid in a porous medium. *Proc. Camb.* **44**, 508–521 (1948)
4. Nield, D.A., Barletta, A.: The Horton–Rogers–Lapwood problem revisited: the effect of pressure work. *Transp. Porous Media* **77**(2), 143–158 (2009)
5. Nield, D.A.: Onset of thermohaline convection in a porous medium. *Water Resour. Res.* **4**(3), 553–560 (1968)
6. Rudraiah, N., Siddheshwar, P.G., Masuoka, T.: Nonlinear convection in porous media: a review. *J. Porous Media* **6**(1), 1–32 (2003)
7. Wollkind, D.J., Frisch, H.L.: Chemical instabilities: I. A heated horizontal layer of dissociating fluid. *Phys. Fluids* (1958–1988) **14**(1), 13–18 (1971a)
8. Wollkind, D.J., Frisch, H.L.: Chemical instabilities. III. Nonlinear stability analysis of a heated horizontal layer of dissociating fluid. *Phys. Fluids* (1958–1988) **14**(3), 482–487 (1971b)
9. Nield, D.A., Bejan, A.: Convection in porous media. Springer (2006)
10. Ingham, D., Pop, I.: Transport phenomenon in porous media, vol. i (1998)
11. Ingham, D.B., Pop, I.: Transport phenomena in porous media III, vol. 3. Elsevier (2005)
12. Vafai, K.: Handbook of porous media. Marcel dekker, New York (2000)
13. Vafai, K.: Handbook of porous media. Crc Press (2005)
14. Vadász, P.: Emerging Topics in Heat and Mass Transfer in Porous Media: From Bioengineering and Microelectronics to Nanotechnology, vol. 22. Springer Science & Business Media (2008)
15. Bdzil, J., Frisch, H.L.: Chemical instabilities. II. Chemical surface reactions and hydrodynamic instability. *Phys. Fluids* (1958–1988) **14**(3), 475–482 (1971)
16. Bdzil, J., Frisch, H.L.: Chemically driven convection. *J. Chem. Phys.* **72**(3), 1875–1886 (1980)
17. Gutkiewicz-Krusin, D., Ross, J.: Rayleigh–Bénard instability in reactive binary fluids. *J. Chem. Phys.* **72**(6), 3577–3587 (1980)
18. Rionero, S.: Long-time behaviour of multi-component fluid mixtures in porous media. *Int. J. Eng. Sci.* **48**(11), 1519–1533 (2010)
19. Rionero, S.: Global nonlinear stability for a triply diffusive convection in a porous layer. *Contin. Mech. Thermodyn.* **24**(4–6), 629–641 (2012)
20. Rionero, S.: Multicomponent diffusive-convective fluid motions in porous layers: Ultimately boundedness, absence of subcritical instabilities, and global nonlinear stability for any number of salts. *Phys. Fluids* (1994–present) **25**(5), 054104 (2013)
21. Rionero, S.: Heat and mass transfer by convection in multicomponent Navier-Stokes Mixtures: Absence of subcritical instabilities and global nonlinear stability via the Auxiliary System Method. *Rendiconti Lincei-Matematica e Applicazioni* **25**(4), 369–412 (2014)
22. Steinberg, V., Brand, H.R.: Convective instabilities of binary mixtures with fast chemical reaction in a porous medium. *J. Chem. Phys.* **78**(5), 2655–2660 (1983)
23. Steinberg, V., Brand, H.R.: Amplitude equations for the onset of convection in a reactive mixture in a porous medium. *J. Chem. Phys.* **80**(1), 431–435 (1984)
24. Gatica, J., Viljoen, H., Hlavacek, V.: Stability analysis of chemical reaction and free convection in porous media. *Int. Commun. Heat Mass Transf.* **14**(4), 391–403 (1987)
25. Gatica, J.E., Viljoen, H.J., Hlavacek, V.: Interaction between chemical reaction and natural convection in porous media. *Chem. Eng. Sci.* **44**(9), 1853–1870 (1989)

26. Viljoen, H.J., Gatica, J.E., Hlavacek, V.: Bifurcation analysis of chemically driven convection. *Chem. Eng. Sci.* **45**(2), 503–517 (1990)
27. Malashetty, M., Gaikwad, S.: Onset of convective instabilities in a binary liquid mixtures with fast chemical reactions in a porous medium. *Heat Mass Transf.* **39**(5–6), 415–420 (2003)
28. Pritchard, D., Richardson, C.N.: The effect of temperature—dependent solubility on the onset of thermosolutal convection in a horizontal porous layer. *J. Fluid Mech.* **571**, 59–95 (2007)
29. Straughan, B.: The energy method, stability, and nonlinear convection. *Applied Mathematical Sciences*, vol. 91, 2nd edn. Springer, New York (2004)
30. Straughan, B.: Stability and wave motion in porous media. *Applied Mathematical Sciences*, vol. 165. Springer, New York (2008)
31. Rionero, S.: Soret effects on the onset of convection in rotating porous layers via the Auxiliary System Method. *Ricerche di Matematica* **62**(2), 183–208 (2013)
32. Capone, F., De Cataldis, V., De Luca, R.: On the nonlinear stability of an epidemic SEIR reaction-diffusion model. *Ricerche di Matematica* **62**(1), 161–181 (2013)
33. Straughan, B.: Nonlinear stability in microfluidic porous convection problems. *Ricerche di Matematica* **63**(1), 265–286 (2014)
34. Capone, F., De Luca, R.: On the stability-instability of vertical throughflows in double diffusive mixtures saturating rotating porous layers with large pores. *Ricerche di Matematica* **63**(1), 119–148 (2014)
35. Rionero, S., Torricollo, I.: Stability of a Continuous Reaction-Diffusion Cournot-Kopel Duopoly Game Model. *Acta Appl. Math.* **132**(1), 505–513 (2014)
36. Capone, F., De Luca, R.: Coincidence between linear and global nonlinear stability of non-constant throughflows via the Rionero Auxiliary System Method. *Meccanica* **49**(9), 2025–2036 (2014)
37. Lombardo, S., Mulone, G.: Induction magnetic stability with a two-component velocity field. *Mech. Res. Commun.* **62**, 89–93 (2014)
38. Rionero, S.: L^2 -energy decay of convective nonlinear PDEs reaction-diffusion systems via auxiliary ODEs systems. *Ricerche di Matematica* **64**(2), 251–287 (2015)
39. De Luca, R.: Global nonlinear stability and cold convection instability of non-constant porous throughflows, 2D in vertical planes. *Ricerche di Matematica* **64**, 99–113 (2015)
40. De Luca, R., Rionero, S.: Convection in multi-component rotating fluid layers via the Auxiliary System Method. *Ricerche di Matematica* 1–17 (2015). doi:[10.1007/s11587-015-0251-y](https://doi.org/10.1007/s11587-015-0251-y)
41. Al-Sulaimi, B.: The energy stability of Darcy thermosolutal convection with reaction. *Int. J. Heat Mass Transf.* **86**, 369–376 (2015)
42. Dongarra, J.J., Straughan, B., Walker, D.W.: Chebyshev tau-QZ algorithm methods for calculating spectra of hydrodynamic stability problems. *Appl. Numer. Math.* **22**(4), 399–434 (1996)
43. Lindsay, K., Straughan, B.: Penetrative convection in a micropolar fluid. *Int. J. Eng. Sci.* **30**(12), 1683–1702 (1992)